# PAR3 and aPKC regulate Golgi organization through CLASP2 phosphorylation to generate cell polarity

Toshinori Matsui, Takashi Watanabe*, Kenji Matsuzawa, Mai Kakeno, Nobumasa Okumura, Ikuko Sugiyama, Norimichi Itoh[†], and Kozo Kaibuchi
Department of Cell Pharmacology, Nagoya University Graduate School of Medicine, Nagoya 466-8550, Japan

**ABSTRACT** The organization of the Golgi apparatus is essential for cell polarization and its maintenance. The polarity regulator PAR complex (PAR3, PAR6, and aPKC) plays critical roles in several processes of cell polarization. However, how the PAR complex participates in regulating the organization of the Golgi remains largely unknown. Here we demonstrate the functional cross-talk of the PAR complex with CLASP2, which is a microtubule plus-end–tracking protein and is involved in organizing the Golgi ribbon. CLASP2 directly interacted with PAR3 and was phosphorylated by aPKC. In epithelial cells, knockdown of either PAR3 or aPKC induced the aberrant accumulation of CLASP2 at the *trans*-Golgi network (TGN) concomitantly with disruption of the Golgi ribbon organization. The expression of a CLASP2 mutant that inhibited the PAR3-CLASP2 interaction disrupted the organization of the Golgi ribbon. CLASP2 is known to localize to the TGN through its interaction with the TGN protein GCC185. This interaction was inhibited by the aPKC-mediated phosphorylation of CLASP2. Furthermore, the nonphosphorylatable mutant enhanced the colocalization of CLASP2 with GCC185, thereby perturbing the Golgi organization. On the basis of these observations, we propose that PAR3 and aPKC control the organization of the Golgi through CLASP2 phosphorylation.

## INTRODUCTION

Cell polarity is a fundamental property of most cell types. Polarized cells distribute their cellular components asymmetrically. This asymmetric organization enables the cells to perform cell-type-specific functions (Drubin and Nelson, 1996; Mellman and Nelson, 2008). In the trafficking required for cell polarity, the Golgi apparatus acts as a sorting center for newly synthesized membrane and proteins, directing them to the functionally specialized domains in the plasma membrane and cytoplasm of polarized cells, such as the leading edge of migrating cells (Kupfer et al., 1982; Bergmann et al., 1983), the developing axon in neurons (Zmuda and Rivas, 1998; de Anda et al., 2005), and the apical or basolateral membranes of epithelial cells (Rodriguez-Boulan et al., 2005; De Matteis and Luini, 2008).

In interphase mammalian cells, the Golgi apparatus itself is a polarized organelle. The Golgi apparatus consists of stacks of flattened cisternae—the Golgi stack—which has *cis* and *trans* faces to allow functionally directional transport (Farquhar and Palade, 1998; Glick and Nakano, 2009). The stacks are assembled, highly ordered, and typically linked, thereby forming a twisted, ribbon-like network—the Golgi ribbon—which retains *cis–trans* polarity for the entire Golgi apparatus (Yadav et al., 2009; Hurtado et al., 2011; Vinogradova et al., 2012). The Golgi ribbon localizes next to the centrosome in the juxtanuclear region (Infante et al., 1999; Takahashi et al., 1999). For polarized post-Golgi trafficking, the Golgi apparatus is reoriented toward and directs its *trans* face at a specific functional region as just described (Li and Gundersen, 2008; Conde and Caceres, 2009; Petrie et al., 2009). Thus the regulation of the polarized organization and orientation of the Golgi apparatus is considered essential for cell polarization.

A PAR complex comprising PAR3, PAR6, and atypical protein kinase C (aPKC) plays a critical role in establishing polarity in various cell types, including front–rear polarity in migrating cells, neuronal polarity, and apicobasal polarity in epithelial cells (Suzuki and Ohno, 2006; Goldstein and Macara, 2007; Etienne-Manneville, 2008; Funahashi et al., 2014). Previous studies investigating the PAR complex in post-Golgi trafficking focused on the microtubule (MT) network and the Golgi orientation in migrating cells, as described later. In various cellular processes, the PAR complex functions cooperatively with Rho-family GTPases, including Cdc42, Rac1, and RhoA (Iden and Collard, 2008). Activated Cdc42 binds to PAR6, which then associates with aPKC and PAR3, leading to the activation of aPKC (Joberty et al., 2000; Lin et al., 2000; Qiu et al., 2000; Garrard et al., 2003). At the leading edge of migrating cells, activated aPKC inactivates GSK-3β, thereby allowing several MT-associated proteins, such as adenomatous polyposis coli (APC), to accumulate at and stabilize MTs; this is followed by the formation of an asymmetric MT network. This MT network, with dynein, induces the relocation of the Golgi toward the leading edge (Etienne-Manneville and Hall, 2001, 2003). During the formation of the PAR complex, PAR3 interacts with the Rac-specific guanine nucleotide exchange factor Tiam1, which is essential for MT stabilization for directional migration (Nishimura et al., 2005; Pegtel et al., 2007). PAR complex formation is disrupted by the RhoA effector Rho-kinase/ROCK through PAR3 phosphorylation (Nakayama et al., 2008). In the wound-healing assay, PAR3 at the cell–cell contacts also relocates the centrosome and the Golgi apparatus anterior to the nucleus via dynein activity (Schmoranzer et al., 2009). Thus the regulatory mechanism of the MT network and the Golgi orientation by the PAR complex has been clarified. In addition, accumulating evidence indicates that the PAR complex controls intracellular trafficking, including endocytosis and exocytosis for cell polarity (Nishimura and Kaibuchi, 2007; Horikoshi et al., 2009; Lalli, 2009; Rosse et al., 2009; Bryant et al., 2010; Harris and Tepass, 2010; Sato et al., 2011; Yoshihama et al., 2011). However, the involvement of the PAR complex in the Golgi apparatus, especially its organization, has not been fully elucidated, but aPKC has been reported to localize to the trans-Golgi network (TGN; Westermann et al., 1996).

The microtubule plus-end–tracking protein (+TIP) cytoplasmic linker–associated protein 2 (CLASP2) and another CLASP isoform, CLASP1, are key regulators of post-Golgi trafficking in cell polarity (Miller et al., 2009). In migrating cells, CLASPs localize at the MT ends and the TGN, depending on the other +TIP end-binding proteins (EBs) and the TGN protein GCC185 (Akhmanova et al., 2001; Mimori-Kiyosue et al., 2005; Efimov et al., 2007; Honnappa et al., 2009). CLASPs at MT ends, which are regionally regulated by GSK-3β, stabilize MTs at the leading edge via linkages to the cell cortex and to actin filaments, thereby contributing to the asymmetry of the MT network (Wittmann and Waterman-Storer, 2005; Drabek et al., 2006; Tsvetkov et al., 2007; Kumar et al., 2009; Watanabe et al., 2009). Meanwhile, CLASPs at the TGN are required for the nucleation of Golgi-derived MTs, most of which are directed toward the leading edge (Efimov et al., 2007). These CLASP-dependent MTs are also necessary for the formation of the Golgi ribbon (Miller et al., 2009). These studies indicate that CLASPs regulate directional trafficking from the Golgi apparatus through the asymmetry of the MT network and the organization of the Golgi ribbon.

In this study, we explored the role of the PAR complex in the regulation of the Golgi apparatus, focusing on CLASP2 as a novel interactor of PAR3. CLASP2 binds directly with PAR3 and is phosphorylated by aPKC. Through CLASP2 phosphorylation, aPKC, together with PAR3, regulates the interaction of CLASP2 with GCC185 and the localization of CLASP2 to the TGN, thereby controlling the organization of the Golgi. On the basis of these findings, we propose a novel molecular mechanism of the PAR complex with CLASP2 for regulating the organization of the Golgi apparatus in cell polarization.

## RESULTS

### PAR3 and CLASP2 form a complex through direct interaction

By comprehensive screening for interactors of PAR3, we previously identified CLASP2 as a candidate interactor (Itoh et al., 2010). We first verified our finding by immunoprecipitating the complex of PAR3 and CLASP2. Endogenous CLASP2 was specifically precipitated with endogenous PAR3 and vice versa (Figure 1A). Furthermore, Myc-fused CLASP2α and CLASP2γ were precipitated with green fluorescent protein (GFP)–fused PAR3 (Figure 1B). CLASP1α was also precipitated with PAR3 (Figure 1C). These results indicate that PAR3 physiologically associates with CLASPs irrespective of its isoforms.

We next characterized the interaction of PAR3 with CLASP2 through a series of biochemical analyses. To narrow down the CLASP2-binding region, we prepared four fragments covering the full length of PAR3 as glutathione S-transferase (GST)–fusion proteins (Figure 1D) and performed pull-down assays. CLASP2 was detected in the eluates of GST–PAR3-2N (amino acids [aa] 252–697) and -4N (aa 937–1337), and more CLASP2 was precipitated with the former PAR3 fragment (Figure 1E). We also found that Myc-PAR3 bound to CLASP2-N2 (aa 310–670) in an immunoprecipitation assay (Figure 1, F and G), indicating that PAR3-2N and CLASP2-N2 are primarily responsible for the interaction between PAR3 and CLASP2. To examine whether this interaction is direct, we then performed an in vitro binding assay using purified GST–PAR3-2N and maltose-binding protein (MBP)–tagged CLASP2-N2. MBP–CLASP2-N2 bound to GST–PAR3-2N in a dose-dependent and saturable manner. Scatchard plot analysis revealed that the $K_d$ value of this interaction was ~6 nM (Figure 1H). These results indicate that PAR3 and CLASP2 form a complex through direct interaction.

### aPKC phosphorylates CLASP2

PAR3 acts as an escort protein for aPKC substrates such as Numb and Tiam1 and is required for their phosphorylation (Nishimura and Kaibuchi, 2007; Wang et al., 2012). We therefore investigated whether aPKC phosphorylates CLASP2. In in vitro phosphorylation assays, aPKCζ and aPKCλ phosphorylated histidine (His)-CLASP2γ but not His-RhoGDI, which was used as a control (Figure 2A and unpublished data). The phosphorylation sites were mapped to the serine/arginine (S/R)-rich and carboxyl (C)-terminal regions in CLASP2 (Supplemental Figure S1A and Figure 2A), which are responsible for its localization to MT ends and the TGN (Akhmanova et al., 2001; Mimori-Kiyosue et al., 2005; Efimov et al., 2007). Because aPKC depletion did not affect its localization to MT ends but did influence its localization to the TGN (see later result), we focused on the phosphorylation of the C-terminal region. aPKCζ phosphorylated GST–CLASP2-C1 (aa 872–1294) but not GST-CLASP2-C (aa 1017–1294; Figure 2B), indicating that aPKC phosphorylation occurs in the region between aa 872 and aa 1016 in CLASP2. To identify the exact phosphorylation site, we prepared a series of CLASP2-C1 point mutants whose potential PKC phosphorylation sites ([S/T]-X-[R/K], [R/K]-X-[S/T] and [R/K]-X-X-[S/T]) in this region were mutated to Ala. Ala substitutions at Ser-940 (S940A), Ser-952 (S952A), and Ser-967 (S967A) significantly reduced the phosphorylation by aPKCζ (Figure 2C), suggesting that these three
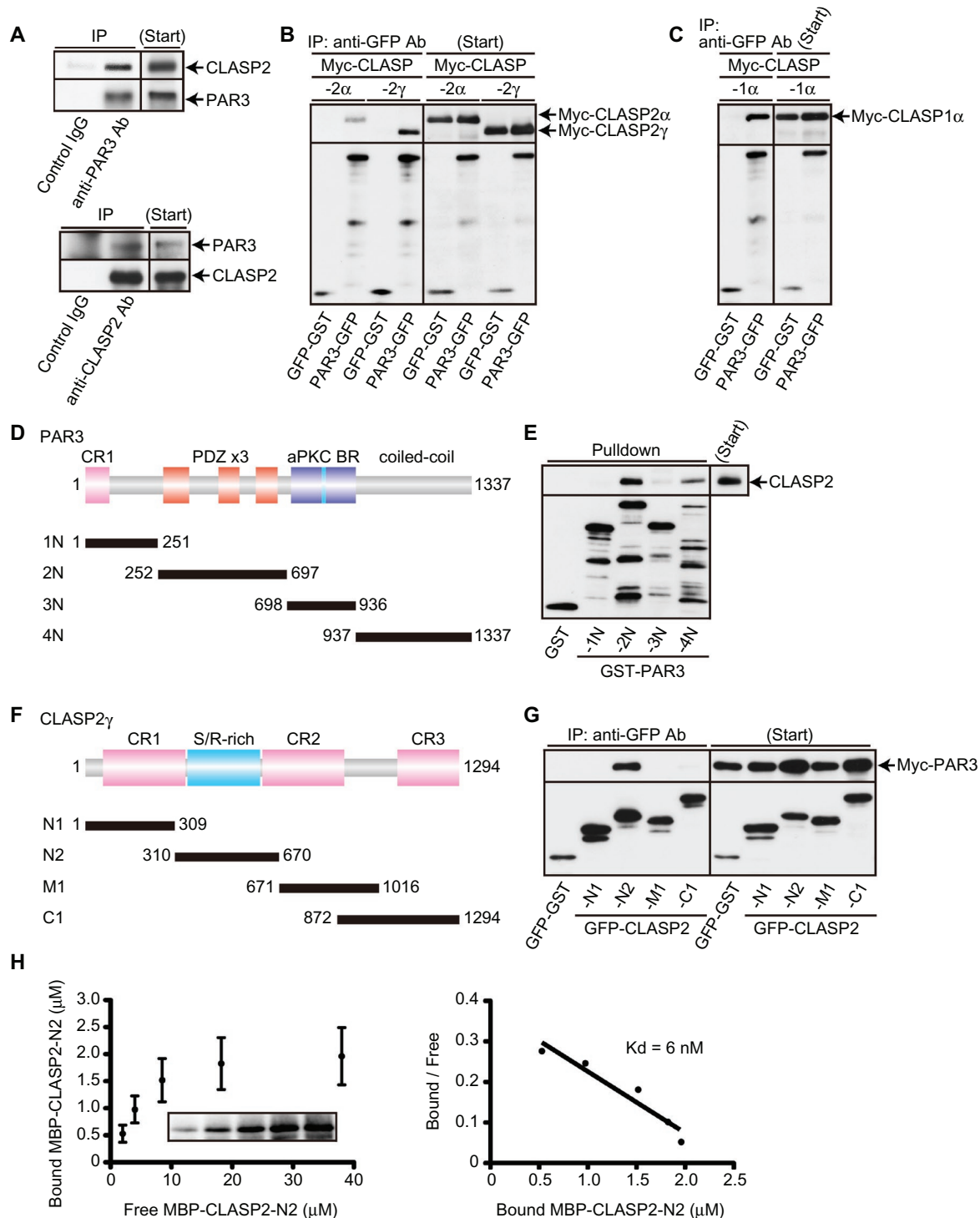
FIGURE 1: PAR3 and CLASP2 form a complex through direct interaction. (A) RPE-1 cell lysates were precipitated with the indicated antibodies. Endogenous PAR3 was specifically coprecipitated with CLASP2 and vice versa. (B, C) Lysates of COS-7 cells expressing PAR3-GFP and Myc-CLASP isoforms were precipitated with anti-GFP antibody. PAR3 formed a complex with each CLASP. (D) The domain structures of PAR3 and its fragments. Numbers refer to amino acids. aPKC BR, aPKC binding region; CR, conserved region; PDZ, PSD95/Discs-Large/ZO-1 domain. (E) Indicated GST-fusion proteins were incubated with lysates from COS-7 cells and precipitated with glutathione beads. CLASP2 was detected in the eluates of GST-PAR3-2N and -4N. (F) Schematic of CLASP2. The domain structures of CLASP2 and its various fragments. CR, conserved region; S/R-rich, serine/arginine-rich. (G) Lysates of COS-7 cells expressing Myc-PAR3 and the indicated GFP-CLASP2 fragments were immunoprecipitated with anti-GFP antibody. Myc-PAR3 was coprecipitated with GFP–CLASP2-N2. (H) Saturable interaction of purified GST–PAR3-2N with MBP–CLASP2-N2. The indicated concentrations of MBP–CLASP2-N2 were incubated with beads coated with GST–PAR3-2N (20 pmol), and the $K_d$ value was calculated by Scatchard analysis. The $K_d$ value of the interaction between PAR3-2N and CLASP2-N2 was ~6 nM. The data represent the means ± SD of more than three independent experiments.
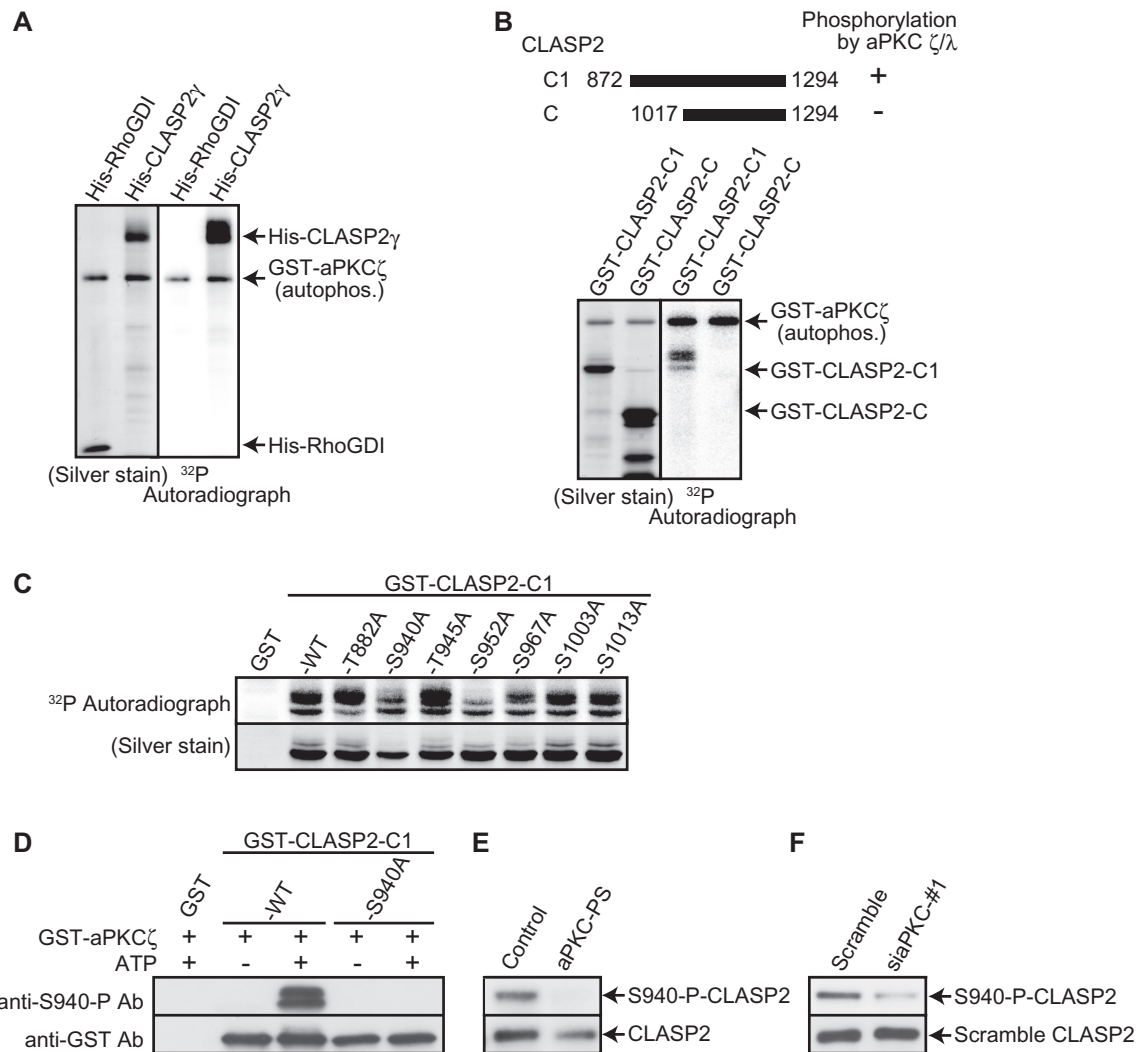
**FIGURE 2:** aPKC phosphorylates CLASP2 both in vitro and in vivo. (A–C) Purified full-length CLASP2γ or its mutants were incubated with recombinant aPKCζ in the presence of [$^{32}$P]ATP, followed by silver staining and autoradiography. (A) aPKC phosphorylated His-CLASP2γ in vitro. (B) Schematic of CLASP2 C-terminal fragments (top). aPKC phosphorylated GST-CLASP2-C1 but not -C (bottom). (C) Ala substitutions at Ser-940 (S940A), Ser-952 (S952A), and Ser-967 (S967A) in CLASP2-C1 reduced the phosphorylation by aPKCζ. (D) GST, GST–CLASP2-C1 wild type (WT), and S940A were incubated with aPKCζ in the presence or absence of ATP, followed by immunoblotting with anti-GST and anti–S940-P antibody. Anti–S940-P antibody detected GST–CLASP2-C1 phosphorylated by aPKCζ but did not detect phosphorylation of the other constructs. (E) RPE-1 cells were incubated with or without 10 μM aPKC pseudosubstrate inhibitor (aPKC-PS) for 20 min, followed by treatment with 100 nM calyculin-A for 10 min. Incubation with aPKC-PS diminished the phosphorylation of Ser-940 in CLASP2. (F) RPE-1 cells transfected with the indicated siRNA were treated with 100 nM calyculin-A for 10 min. aPKC depletion reduced the phosphorylation of Ser-940 in CLASP2. All results are representative of three independent experiments.

Ser residues are major sites of phosphorylation by aPKC. To verify the in vivo phosphorylation of CLASP2, we attempted to generate phosphospecific antibodies against these residues and successfully produced anti–S940-P antibody. In immunoblot analysis, anti–S940-P antibody detected the phosphorylation of CLASP2-C1 by aPKCζ in vitro but not that of CLASP2-C1-S940A (Figure 2D), indicating that anti–S940-P antibody specifically detects the Ser-940 phosphorylation of CLASP2. This antibody did not detect the phosphorylation of endogenous CLASP2 in RPE-1 cells under normal growth conditions. However, treatment of the cells with calyculin-A, a phosphatase inhibitor for PP1 and PP2A, increased the phosphorylation level of CLASP2, and this increase was suppressed by pretreatment with an aPKC pseudosubstrate inhibitor (aPKC-PS; Figure 2E) and

depletion of aPKC (Figure 2F; see later result). Under the same condition, depletion of PAR3 also reduced the phosphorylation of Ser-940 in CLASP2 (unpublished data). Because the phosphorylation levels of the proteins are regulated by the balance between kinases and phosphatases, these results suggest that aPKC, together with PAR3, phosphorylates CLASP2 in vivo and that the turnover of this phosphorylation is rapid.

## PAR3 and aPKC cooperatively regulate the localization of CLASP2 to the TGN and the organization of the Golgi ribbon

CLASPs accumulate at the Golgi apparatus and the plus ends of MTs, depending on GCC185 and EBs (Mimori-Kiyosue et al.,
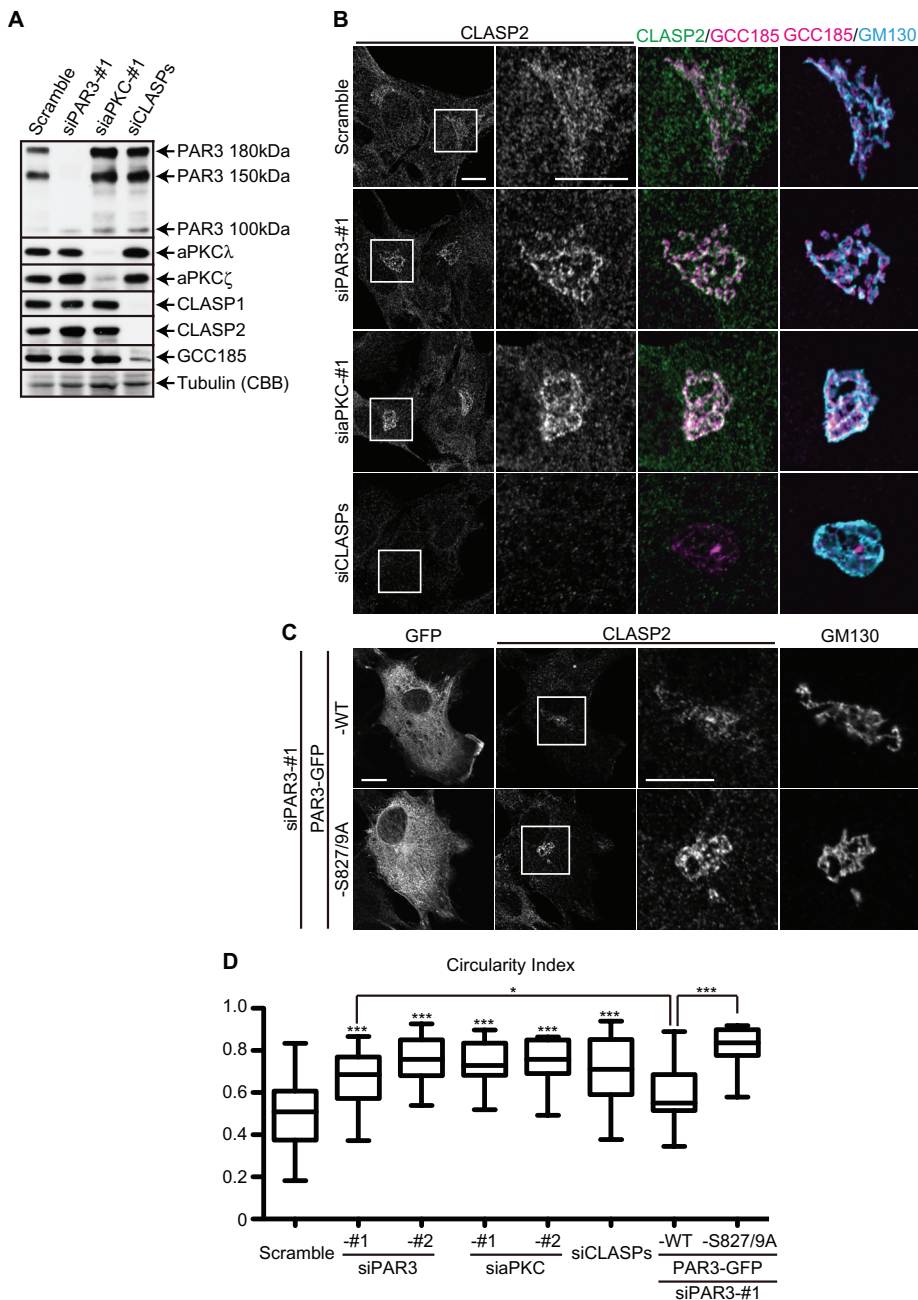
**FIGURE 3:** PAR3 and CLASP2 cooperatively regulate the localization of CLASP2 to the TGN and the organization of the Golgi ribbon. (A) RPE-1 cells were transfected with indicated siRNA, followed by immunoblotting. The transfection of siRNAs reduced the expression of their respective target proteins to undetectable levels. CBB, Coomassie Brilliant Blue staining. (B) RPE-1 cells transfected with the indicated siRNAs were fixed with methanol at −30°C for 20 min, followed by immunostaining with CLASP2 (gray and green), GCC185 (magenta), and GM130 (cyan). Depletion of PAR3 and aPKC increased CLASP2 at the TGN, enhanced the colocalization of CLASP2 and GCC185, and disrupted the organization of the Golgi ribbon. Right, magnifications of left insets. Bars, 10 μm. (C) Rescue experiments for CLASP2 localization and the Golgi ribbon organization. RPE-1 cells were transfected with siRNA for PAR3 along with the indicated plasmids. These cells were fixed with methanol at −30°C for 20 min, followed by immunostaining with anti-GFP, anti-CLASP2, and anti-GM130 antibodies. The expression of siRNA-resistant PAR3-GFP partially restored CLASP2 localization and the organization of the Golgi ribbon, but expression of PAR3-S827/9A, which is defective in aPKC binding, failed to do so. Right, magnifications of left insets. Bars, 10 μm. (D) The circularity index of the Golgi morphology was calculated (see *Materials and Methods*). $n > 30$. *$p < 0.05$, ***$p < 0.001$. All results are representative of three independent experiments.

2005; Efimov *et al.*, 2007). We used RNA interference to examine whether PAR3 and aPKC participate in the localization of CLASP2 in RPE-1 cells. Because RPE-1 cells are supposed to express CLASP2α and its N-terminal truncated alternative isoform CLASP2γ, we used small interfering RNA (siRNA) targeting their common sequence to deplete both isoforms (Akhmanova *et al.*, 2001; Mimori-Kiyosue *et al.*, 2005; Miller *et al.*, 2009; Watanabe *et al.*, 2009). Depletion of PAR3, aPKC, or CLASPs in RPE-1 cells with siRNA was confirmed by immunoblot analysis (Figure 3A and Supplemental Figure S2). Depletion of CLASPs also reduced the level of GCC185 to ~25.3% of that in control cells. CLASP2 accumulated at the Golgi apparatus and partially overlapped with GCC185 in scramble-transfected cells (Figure 3B), as previously described (Efimov *et al.*, 2007). Those cells displayed tightly packed and elongated intact Golgi morphology—Golgi ribbons—judging by the fluorescence of the *cis*-Golgi protein GM130. However, depletion of CLASPs diminished the signal of CLASP2 and changed the Golgi ribbon morphology into a circular appearance (Miller *et al.*, 2009). Under the same conditions, depletion of PAR3 and aPKC increased the accumulation of CLASP2 at the TGN and enhanced the colocalization of CLASP2 and GCC185 concomitantly with disruption of the Golgi ribbon (Figure 3B). On the basis of the method described in Miller *et al.* (2009), we quantified the disruption of the Golgi ribbon by measuring the circularity index of the Golgi. Depletion of PAR3 and aPKC increased the circularity of the Golgi ribbon (Figure 3D). Of note, depletion of PAR3 and aPKC did not noticeably affect the localization of CLASP2 at the plus ends of microtubules under this condition (unpublished data).

To test whether PAR3 and aPKC cooperate to regulate the localization of CLASP2 and the organization of the Golgi, we performed a rescue experiment in the PAR3-depleted cells. The expression of siRNA-resistant PAR3-GFP partially restored the localization of CLASP2 and the organization of the Golgi ribbon, whereas the expression of PAR3-S827/9A, which is defective in aPKC binding (Nagai-Tamai *et al.*, 2002; Horikoshi *et al.*, 2009), failed to rescue those phenotypes (Figure 3, C and D). These results indicate that PAR3 and aPKC cooperatively regulate the localization of CLASP2 to the TGN and the organization of the Golgi ribbon.

**A** CLASP2γ

| | Interaction with PAR3-2N | -4N | EB1 | IQGAP1 |
|---|---|---|---|---|
| 1 — 1294 (CR1, S/R-rich, CR2, CR3) | + | + | + | + |
| N2  310 — 670 | + | + | + | + |
| N2-1  481 — 550 | + | + | + | − |
| DN  481 — 550 | + | + | − | − |

*: EB binding motif

**B**

GFP-CLASP2γ

GST | GST-PAR3-2N | GST | GST-PAR3-4N | (20 nM)

**C**

HA | CLASP2 | GM130

HA-CLASP2-N1 / HA-CLASP2-DN

**D**

HA | GCC185/GM130

Circularity Index

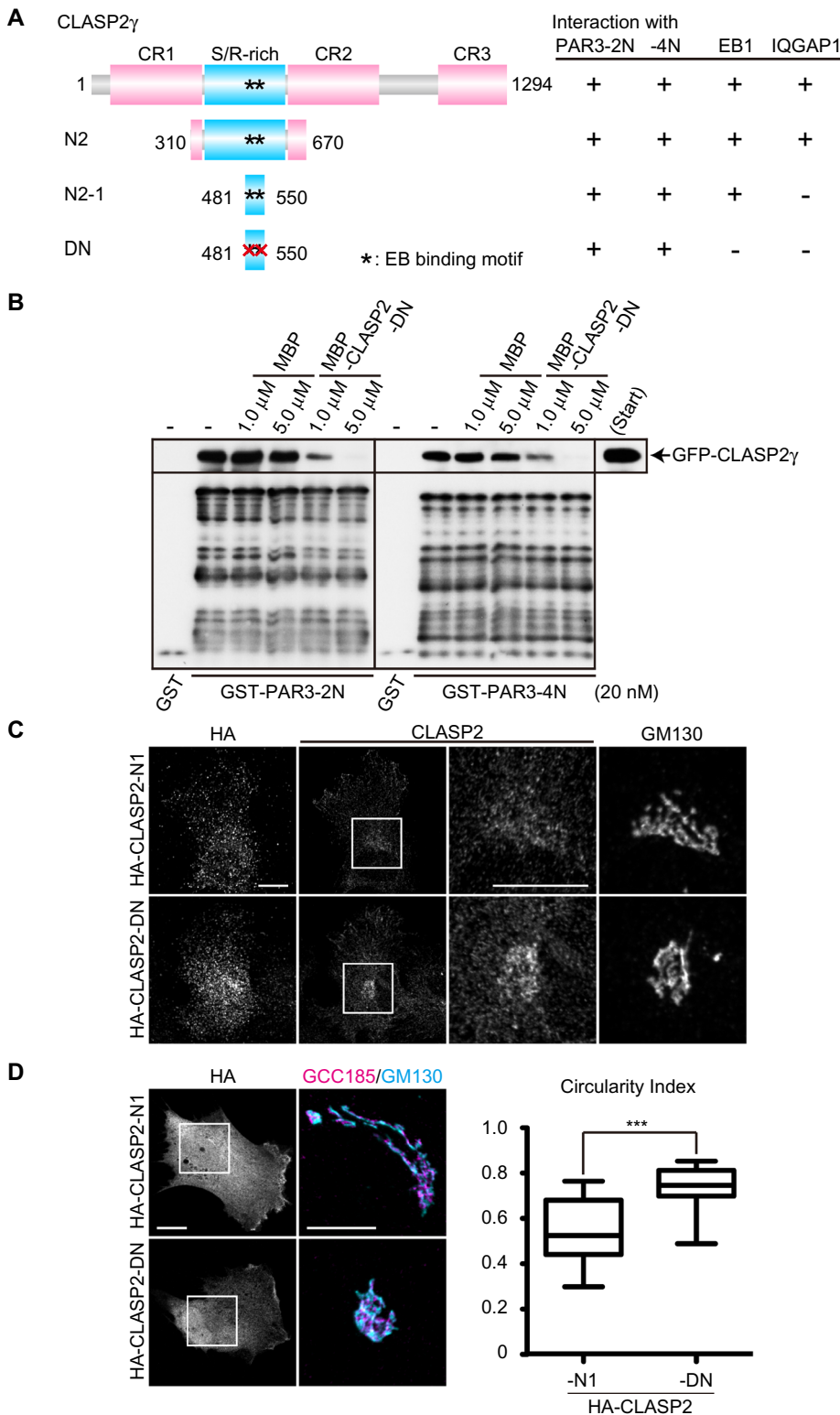HA-CLASP2-N1 / HA-CLASP2-DN

***

HA-CLASP2: -N1, -DN

FIGURE 4: The interaction of CLASP2 with PAR3 is essential for the organization of the Golgi ribbon. (A) Schematic presentation of CLASP2 mutants and their binding abilities to PAR3-2N, -4N, EB1, and IQGAP1. CLASP2-DN bound to PAR3-2N and -4N but neither EB1 nor IQGAP1 (see Supplemental Figure S3). Asterisks indicate the locations of EB-binding motif. The red X indicates the mutation site in EB-binding motif. (B) GST- or GST-PAR3-2N– or -4N–immobilized beads were incubated with COS-7 cell lysates expressing GFP-CLASP2γ in the presence or absence of MBP-fusion proteins. The bound proteins were analyzed by immunoblotting. Increasing amounts of MBP–CLASP2-DN inhibited the interaction of CLASP2 with PAR3-2N and -4N. (C) To examine the effect of the expression of CLASP2-DN on CLASP2 localization, RPE-1 cells expressing HA–CLASP2-N1 or -DN were fixed with methanol at −30°C for 20 min, followed

**The interaction between PAR3 and CLASP2 is essential for Golgi ribbon organization**

To examine whether the PAR3-CLASP2 interaction regulates the localization of CLASP2 to the TGN and the organization of the Golgi ribbon, we attempted to generate a CLASP2 mutant that inhibits the PAR3-CLASP2 interaction in a dominant-negative manner. Because the CLASP2-N2 region is also responsible for interacting with EBs, IQGAP1, and MTs (Mimori-Kiyosue et al., 2005; Watanabe et al., 2009), we sought to identify the CLASP2 region that specifically interacted with PAR3. CLASP2-N2-1 (aa 481–550) bound to PAR3-2N and -4N but not to IQGAP1 (Figure 4A and Supplemental Figure S3). CLASP2-N2-1 has two EB-binding motifs (Ser-X-Ile-Pro; Honnappa et al., 2009), and replacement of the Ile-Pro with Ser-Ser impaired the interaction with EB1 but had no effect on the interactions with PAR3-2N and -4N (Figure 4A and Supplemental Figure S3). These results indicate that the CLASP2-N2-1 mutant that is defective in EB-binding, called CLASP2-DN, specifically interacts with PAR3. MBP–CLASP2-DN inhibited the interaction of CLASP2 with GST–PAR3-2N or -4N in a dose-dependent manner (Figure 4B). Thus CLASP2-DN appears to function as a dominant-negative mutant by competing with the PAR3-CLASP2 binding. The expression of hemagglutinin (HA)–CLASP2-DN in RPE-1 cells increased the accumulation of CLASP2 at the TGN concomitantly with disruption of the Golgi ribbon, whereas that of HA–CLASP2-N1, used as a control, had little effect (Figure 4, C and D). The analysis of the circularity index of the Golgi confirmed that the CLASP2-DN expression significantly disrupted the Golgi ribbon morphology (Figure 4D). These results suggest that the PAR3-CLASP2 interaction regulates the

by immunostaining with anti-HA, anti-CLASP2, and anti-GM130 antibodies. The ectopic expression of CLASP2-DN increased the accumulation of CLASP2 at the Golgi apparatus. Bars, 10 μm. (D) To monitor the expression level of CLASP2-DN and examine its effect on the Golgi organization, the indicated RPE-1 cells were fixed with 2% paraformaldehyde and permeabilized with 0.2% Triton X-100, followed by immunostaining with anti-HA (gray), anti-GCC185 (magenta), and anti-GM130 (cyan). Bars, 10 μm. Right, graph of circularity index of the Golgi morphology in indicated cells. The ectopic expression of CLASP2-DN induced the circular appearance of the Golgi. n > 30. ***p < 0.001. All results are representative of three independent experiments.
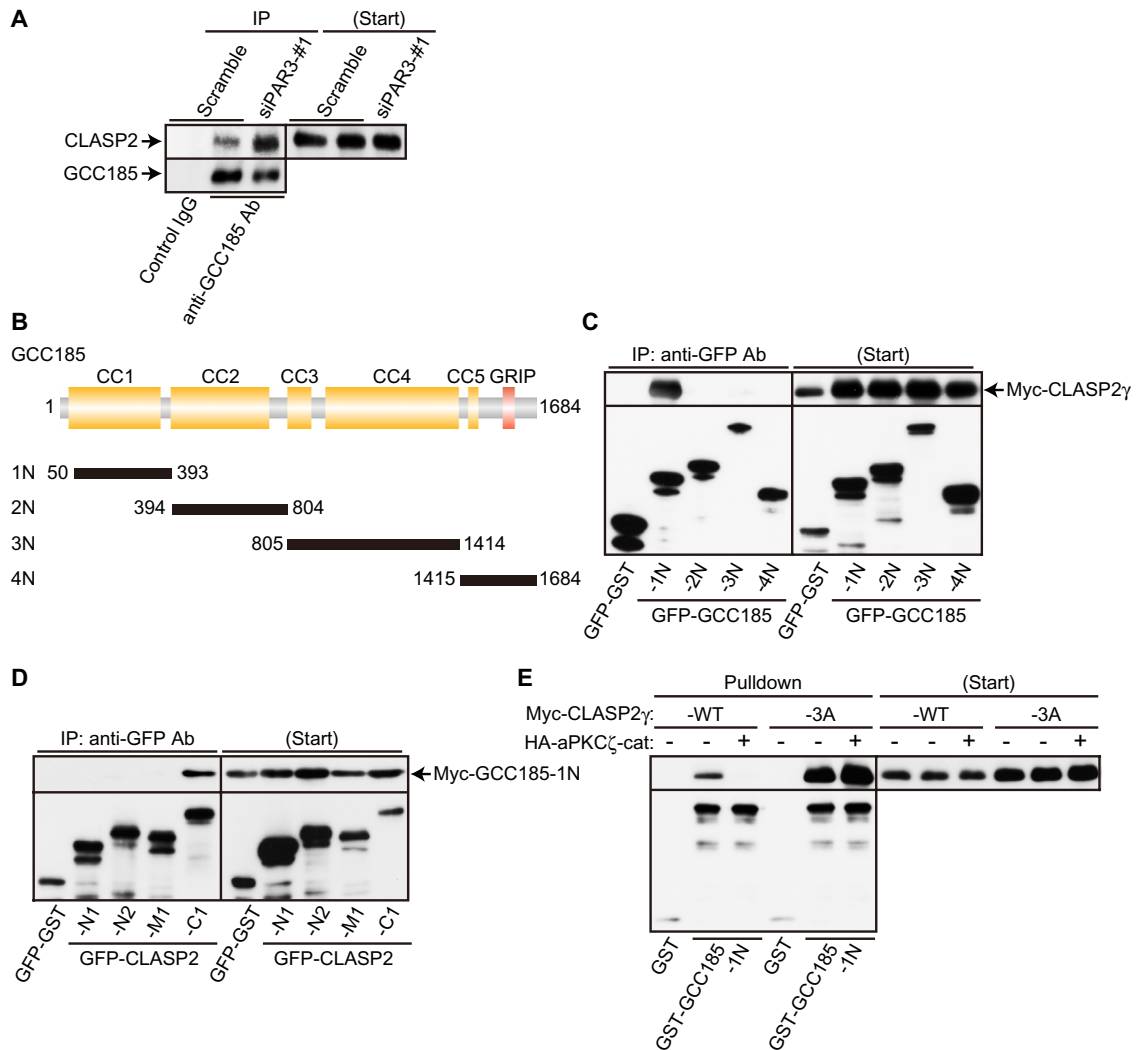
**FIGURE 5:** PAR3 and aPKC regulate the interaction of CLASP2 with GCC185. (A) Control and PAR3-depleted RPE-1 cells were cross-linked with 1 mM DSP, followed by precipitation with anti-GCC185 antibody. Depletion of PAR3 increased the association between CLASP2 and GCC185. (B) The domain structures of GCC185 and its fragments. CC, Coiled-coil domain; GRIP, GRIP domain. (C, D) Lysates of COS-7 cells expressing indicated Myc-fusion proteins and GFP-fusion proteins were immunoprecipitated with anti-GFP antibody. Myc-CLASP2γ was coprecipitated with GFP–GCC185-1N (C), and Myc–GCC185-1N was coprecipitated with GFP–CLASP2-C1 (D). (E) COS-7 cells were transfected with the indicated constructs, and their lysates were pulled down with GST–GCC185-1N. The coexpression of aPKCζ catalytic kinase domain (aa 226–592, aPKCζ-cat) impaired the interaction of GCC185-1N with CLASP2γ-WT but not with -3A. All results are representative of three independent experiments.

localization of CLASP2 to the TGN and the organization of the Golgi ribbon.

## PAR3 and aPKC regulate the interaction of CLASP2 with GCC185

To explore the mechanism regulating the localization of CLASP2 to the TGN dependent on PAR3 and aPKC, we examined the involvement of PAR3 and aPKC in the interaction between CLASP2 and GCC185. On the basis of a previous report (Lin *et al.*, 2011), we used dithiobis succinimidyl propionate (DSP) as a cross-linker for the immunoprecipitation of endogenous CLASP2-GCC185 complex. Under the condition in which CLASP2 was coprecipitated with GCC185 from control cells, PAR3 depletion increased the amount of CLASP2 coprecipitated with GCC185 (Figure 5A), suggesting that PAR3 negatively regulates the interaction between CLASP2 and GCC185. The effects of aPKC depletion were inconclusive because the treatment

of the cross-linker with aPKC-depleted cells drastically decreased the GCC185 solubility for the immunoprecipitation.

To examine whether aPKC regulates the interaction between CLASP2 and GCC185, we used a pull-down assay with GST-fused GCC185-1N, which was proved to be the CLASP2- binding region in the immunoprecipitation assay (Figure 5, B and C). Myc-CLASP2γ was pulled down with GST–GCC185-1N, whereas the coexpression of HA-tagged aPKCζ catalytic kinase domain (aa 226–592, aPKCζ-cat) inhibited this interaction (Figure 5E), indicating that aPKC inhibits the CALSP2-GCC185 interaction. We further examined whether this inhibition by aPKC depends on the phosphorylation of CLASP2. Because of two regions phosphorylated by aPKC, the CLASP2-N2 and -C1 regions, GCC185 bound to the latter (Figure 5D), we used the C-terminal region for further experiments. In pull-down assays with the CLASP2-3A mutant in which three aPKC phosphorylation sites (Ser-940, Ser-952, and Ser-967) in the C-terminal region were
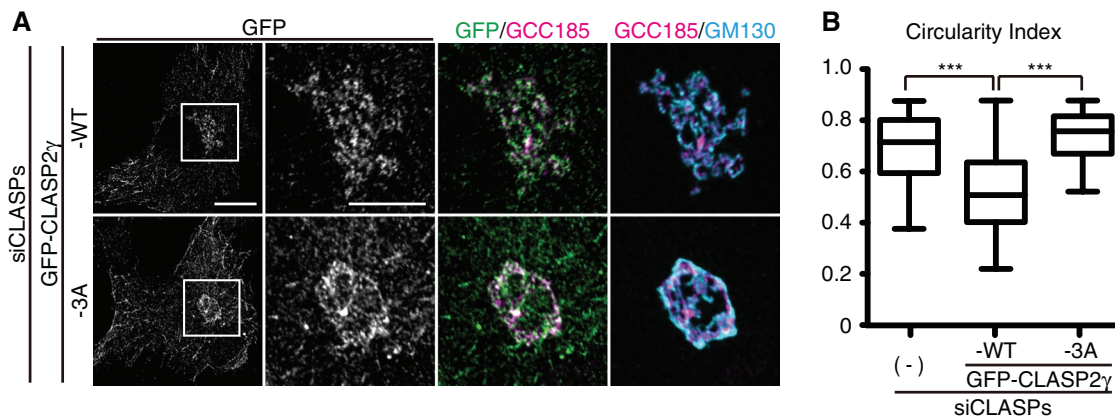
**FIGURE 6:** CLASP2 phosphorylation by aPKC is essential for Golgi ribbon organization. (A) Rescue experiments for Golgi ribbon organization. RPE-1 cells were transfected with siRNA for CLASPs along with the indicated plasmids. These cells were fixed with methanol at −30°C for 20 min, followed by immunostaining with anti-GFP (gray and green), anti-GCC185 (magenta), and anti-GM130 (cyan) antibodies. The expression of siRNA-resistant CLASP2γ-WT restored Golgi ribbon organization, but CLASP2-3A failed to do so. Right, magnifications of left insets. Bars, 10 μm. (B) Circularity index of the Golgi morphology in indicated cells. $n > 40$. ***$p < 0.001$. All results are representative of three independent experiments.

simultaneously mutated into Ala, the mutant was precipitated with GCC-185-1N to a similar extent to wild type, irrespective of the presence of aPKCζ-cat (Figure 5E). These results indicate that aPKC inhibits the interaction of CLASP2 with GCC185 through the phosphorylation of the CLASP2 C-terminal region.

## CLASP2 phosphorylation by aPKC is essential for the organization of the Golgi ribbon

Finally, we performed rescue experiments in CLASP-depleted cells with GFP–CLASP2γ-3A. The expression of the siRNA-resistant wild-type CLASP2γ restored the organization of the Golgi ribbon to that observed in control cells. However, GFP–CLASP2γ-3A failed to restore the organization of the Golgi ribbon (Figure 6, A and B). In addition, compared with the wild type, GFP–CLASP2γ-3A strongly colocalized with GCC185, which was similar to the behavior of endogenous CLASP2 in PAR3- and aPKC-depleted cells (Figures 3B and 6A). These results suggest that PAR3 and aPKC regulate the organization of the Golgi ribbon through the phosphorylation of CLASP2.

## DISCUSSION
### The PAR complex regulates the organization of the Golgi through CLASP2 for directional trafficking

Accumulating evidence suggests the involvement of the PAR complex in directional trafficking in polarized cells. In migrating epithelial cells, the Golgi apparatus is a center of directional trafficking, and its regulation leads to the formation of the polarity axis. Previous studies revealed that the PAR complex orients the Golgi apparatus toward the leading edge through the asymmetric MT network for directional trafficking. Here we found that depletion of PAR3 and inhibition of aPKC induced aberrant accumulation of CLASP2 at the TGN, resulting in the disruption of the Golgi ribbon organization (Figures 3 and 6). Regulation of the Golgi organization is also essential for directional trafficking from the Golgi apparatus. The disruption of the organization of the Golgi by depolymerizing MTs or depletion of Golgi proteins does not affect the intra-Golgi transport or overall secretion to the plasma membrane, but it impairs the directional trafficking (Miller *et al.*, 2009; Yadav *et al.*, 2009; Hurtado *et al.*, 2011), which is most likely caused by the disorganization in the overall *cis–trans* polarity of the Golgi ribbon, although each individual Golgi stack retains its *cis–trans* polarity (Cole *et al.*, 1996;

Lowe, 2011; Vinogradova *et al.*, 2012). Consistently, depletion of PAR3 and the inhibition of aPKC appeared to disrupt the overall *cis–trans* polarity of the Golgi ribbon (Figures 3 and 6). Furthermore, cisternal unstacking and remodeling are required for the reorientation of the Golgi apparatus and centrosome (Bisel *et al.*, 2008). Our studies, together with these findings, suggest that the PAR complex orchestrates the reorientation and organization of the Golgi apparatus for directional trafficking. In concert with the reorientation of the Golgi, the PAR complex may accelerate the Golgi dynamics by regulating CLASP2 accumulation at the TGN downstream of Cdc42 or other factors (see later discussion).

### Regulation of CLASP2 localization to the TGN by the PAR complex

CLASPs are key regulators of directional trafficking from the Golgi apparatus, thereby establishing and maintaining cell polarity. CLASPs localize to the TGN and regulate the organization of the Golgi ribbon. At the TGN, CLASPs stabilize MTs and anchor these MTs to the TGN membrane through GCC185, contributing to Golgi-derived MT nucleation, which is required for Golgi ribbon formation (Efimov *et al.*, 2007; Miller *et al.*, 2009). Both the formation and the maintenance of the Golgi depend on MTs (Cole *et al.*, 1996; Chabin-Brion *et al.*, 2001; Shorter and Warren, 2002). The Golgi structure, especially the TGN, is dynamically regulated for both post-Golgi trafficking and Golgi reorientation (Bisel *et al.*, 2008; De Matteis and Luini, 2008; Sengupta and Linstedt, 2011). However, the regulation of CLASPs at the TGN remains unclear. In this study, we reveal novel roles for the PAR complex in localizing CLASP2 to the TGN in the Golgi apparatus. aPKC and PAR3 inhibit the interaction of CLASP2 with GCC185 by phosphorylating CLASP2 (Figure 5), thereby regulating CLASP2 localization to the TGN. This regulation of CLASP2 localization to the TGN is required for the correct organization of the Golgi ribbon (Figures 3 and 6). On the basis of these findings, we speculate that CLASP2 phosphorylation by aPKC promotes the turnover of CLASP2 at the TGN, thereby facilitating the dynamic nature of the MT-TGN linkage and ensuring that the Golgi structure remains dynamic. This Golgi dynamicity might contribute to the remodeling for the Golgi reorientation, as well as to the maintenance of the overall *cis–trans* polarity of the Golgi ribbon, for directional trafficking from the Golgi apparatus.

## Regulation of the PAR complex at the Golgi apparatus

The PAR complex is activated downstream of migratory stimuli such as integrin engagement to extracellular matrix through Cdc42, which is required for the reorientation of the Golgi apparatus, as described earlier in this article (Etienne-Manneville and Hall, 2001; Iden and Collard, 2008). In other cellular processes, including endocytosis and exocytosis for cell polarity, the PAR complex acts as a Cdc42 effector (Martin-Belmonte et al., 2007; Harris and Tepass, 2010), suggesting that Cdc42 plays a central role in cell polarization in conjunction with the PAR complex. Cdc42 localizes to the Golgi apparatus (Erickson et al., 1996; Fukata et al., 2003). The GTP/GDP cycling of Cdc42 at the Golgi apparatus appears to be essential for the organization of the Golgi ribbon (Chen et al., 2005; Dubois et al., 2005). At the *cis* side of the Golgi, Cdc42 and its effectors regulate the Golgi-to-endoplasmic reticulum transport (Wu et al., 2000; Luna et al., 2002; Matas et al., 2004). At the *trans* side, Cdc42 is activated (Nalbant et al., 2004; Egorov et al., 2009) and is involved in the sorting of vesicles from the TGN to the plasma membrane in the apicobasal polarity of epithelial cells (Kroschewski et al., 1999; Cohen et al., 2001; Musch et al., 2001). However, the mode of action of Cdc42 at the *trans* side is not fully elucidated. It is tempting to speculate that Cdc42 is involved in the post-Golgi trafficking for cell polarity through the regulation of the PAR-CLASP complex.

## MATERIALS AND METHODS

### Reagents and chemicals

The anti-CLASP2 antibody and the anti-PAR3 antibody were described previously (Nishimura et al., 2005; Watanabe et al., 2009). Anti–S940-P-CLASP2 polyclonal antibody was raised against the phosphopeptide (EDIYSS(-P)LRGVT; Sigma-Aldrich, St. Louis, MO) and affinity purified against the phosphopeptide. The anti-GCC185 antibody was kindly provided by Suzanne R. Pfeffer (Stanford University, Stanford, CA). The following commercial antibodies were used: anti-PAR3 (Millipore, Billerica, MA), anti-aPKCλ (BD Biosciences, San Jose, CA), anti-aPKCζ (Santa Cruz Biotechnology, Santa Cruz, CA), anti-CLASP2, anti-CLASP1, and anti-GCC2 (Abcam, Cambridge, MA), anti-GM130 (BD Biosciences), anti-GFP (Roche Diagnostics, Basel, Switzerland; MBL, Nagoya, Japan; Nacalai Tesque, Kyoto, Japan), anti-GST (Sigma-Aldrich), anti-Myc (9E10; purified in-house from hybridoma), and anti-HA (12CA5; purified in-house from hybridoma and 3F10, Roche Diagnostics). The following siRNAs from Sigma-Aldrich were used: Control Scramble, 5′-CAGU-CGCGUUUGCGACUGG-3′; siPAR3-#1, 5′-GGCAUGGAGACCUUG-GAAG-3′; siPAR3-#2, 5′-GAAUGUAUUUAGUACGACU-3′; siCLASP1-a, 5′-GCCAUUAUGCCAACUAUCU-3′; siCLASP2-a, 5′-GACAUA-CAUGGGUCUUAGA-3′; siCLASP1-b, 5′-GGAUGAUUUACAAG-ACUGG-3′; siCLASP2-b, 5′-GUUCAGAAAGCCCUUGAUG-3′; siaPKCλ-#1, 5′-CGAACAGCUCUUCACCAUG-3′; siaPKCζ-#1, 5′-AGAGGAUCGACCAGUCAGA-3′; siaPKCλ-#2 5′-CUUUCCAA-GCCAAGCGUUU-3′; and siaPKCζ-#2, 5′-GAUUGACCCUUUAACU-GUA-3′. For depletion of CLASP and aPKC, we used a mixture of appropriate siRNAs. GST-aPKCζ used for phosphorylation assay was obtained from CARNA Bioscience (Kobe, Japan). The aPKC pseudo-substrate inhibitor was provided by Calbiochem (San Diego, CA). Other chemicals were obtained from commercial sources.

### Plasmid constructions

The cDNAs encoding PAR3, CLASP1, and CLASP2 were obtained as described previously (Nishimura et al., 2005; Watanabe et al., 2009). GCC185 cDNA was kindly provided by Paul A. Gleeson (University of Melbourne, Melbourne, Australia). aPKCζ cDNA was obtained

from Kazusa DNA Research Institute (Chiba, Japan), and its catalytic kinase domain (aPKCζ-cat, aa 226–592) was used. Fragments of cDNA were amplified using PCR and subcloned into the pGEX (GE Healthcare Bio-Sciences, Uppsala, Sweden), pEGFP (Takara Bio, Otsu, Japan), pCAGGS-Myc, and pCAGGS-HA vectors. For the rescue experiments, siRNA-resistant CLASP2 and PAR3 harboring mutations in the siRNA target sequences were as described previously (Nishimura et al., 2005; Watanabe et al., 2009). PAR3 or CLASP2 alanine mutations were generated with a site-directed mutagenesis kit (Stratagene, Santa Clara, CA).

### Cell culture and transfection

COS-7 cells were cultured in DMEM with 10% fetal bovine serum (FBS), and hTERT RPE-1 cells (American Type Culture Collection, Manassas, VA) were maintained in DMEM/F12 with 10% FBS. COS-7 cells were transfected with Lipofectamine 2000 (Invitrogen, Carlsbad, CA) according to the manufacturer's protocol, and RPE-1 cells were transfected with X-tremeGENE HP (Roche Diagnostics) according to the manufacturer's protocol. For siRNA transfection, Lipofectamine RNAiMAX (Invitrogen) was used.

### Protein purification and biochemistry

Recombinant proteins were produced in *Escherichia coli* (XL-1 Blue, BL21DE3, or RosettaDE3) and purified as described previously (Kakeno et al., 2014). Briefly, the collected bacteria were suspended and sonicated. After ultracentrifugation for 1 h at $100,000 \times g$, the supernatants were applied to the columns containing glutathione–Sepharose for GST fusions (GE Healthcare Bio-Sciences). After washing of the columns, the proteins were eluted with the buffer containing reduced glutathione, and they were then dialyzed against the appropriate buffer. All protein purification procedures were performed at 4°C.

### Pull-down and immunoprecipitation assays

For the pull-down assay, transfected COS-7 cells were washed with phosphate-buffered saline (PBS) and lysed with buffer A (20 mM Tris/HCl, pH 7.5, 1% NP-40, 50 mM NaCl, protease inhibitors). After removal of debris by centrifugation, the lysates were incubated with 20 pmol of GST-fusion proteins and glutathione beads for 1 h at 4°C. The beads were washed with buffer A and dissolved in SDS sample buffer. In the immunoprecipitation assay, appropriate antibodies and Protein A Sepharose (GE Healthcare Bio-Sciences) were used instead of GST-fusion proteins and glutathione beads. The immunoprecipitation assay for endogenous GCC185-CLASP2 complex was described elsewhere (Lin et al., 2011) and was performed with some modifications. Briefly, RPE-1 cells were cross-linked with 1 mM DSP (Pierce Biotechnology, Rockford, IL) for 15 min before lysis.

### In vitro binding assay

The in vitro binding assay was performed as described previously (Watanabe et al., 2009). Briefly, purified MBP-tagged CLASP2-N2 was mixed with affinity beads coated with GST–PAR3-2N in buffer A. The beads were then washed with buffer A, and the bound proteins were eluted with buffer A containing 10 mM reduced glutathione. The eluates were subjected to SDS–PAGE, followed by immunoblot analysis using an anti-MBP antibody. The amount of CLASP2-N2 bound to GST-PAR3-2N was detected in a linear range using serial dilutions of standards by chemiluminescent detection and estimated with a Densitograph (ATTO, Tokyo, Japan) or with the ImageQuant LAS 4010 (GE Healthcare Bio-Sciences). Purified CLASP2-N2 was used as the standard for quantification.

## In vitro phosphorylation assay

The kinase reaction was conducted in 50 µl of kinase buffer (50 mM Tris-HCl, pH 7.5, 5 mM MgCl$_2$, 0.3 mM dithiothreitol) containing 100 µM [γ-$^{32}$P]ATP, 40 ng/µl recombinant kinases (GST-aPKCζ or GST-aPKCλ-cat), and 1 µM substrate (purified His- or GST-fusion proteins). After incubation for 2 h at 30°C, the reaction mixtures were boiled in SDS sample buffer and subjected to SDS–PAGE and silver staining. The radiolabeled bands were visualized with an image analyzer (Typhoon FLA 9000; GE Healthcare Bio-Sciences).

## Immunohistochemical analysis

The cells were fixed with methanol at –30°C for 20 min or with 2% paraformaldehyde for 20 min, followed by permeabilization with 0.2% Triton X-100. After incubation with blocking buffer (0.2% Tween-20, 1 mg/ml bovine serum albumin, PBS) for 60 min at room temperature, the cells were incubated overnight at 4°C with the indicated primary antibodies and for 1 h at room temperature with the indicated secondary antibodies. The cells were observed using a 1.4 numerical aperture CFI Plan-Apo VC 60× or Plan-Apo 63× oil immersion objective lens under a confocal laser microscope (LSM780; Carl Zeiss, Jena, Germany).

To quantify the disruption of the Golgi ribbon, the circularity index of the Golgi morphology was measured as described elsewhere (Miller *et al.*, 2009). Briefly, a freehand selection option in ImageJ software (National Institutes of Health, Bethesda, MD) was used to outline the Golgi based on GM130 staining. Circularity index values were assigned to Golgi outlines by the ImageJ circularity plug-in (http://rsb.info.nih.gov/ij/plugins/circularity.html), where circularity = $4\pi$(area/perimeter$^2$). A circularity value of 1 corresponds to a perfect circle.

## Statistical analysis

Statistical analyses were performed with Prism, version 5.0 (GraphPad Software, La Jolla, CA). $p < 0.05$ was considered to indicate statistical significance.

## REFERENCES

Akhmanova A, Hoogenraad CC, Drabek K, Stepanova T, Dortland B, Verkerk T, Vermeulen W, Burgering BM, De Zeeuw CI, Grosveld F, Galjart N (2001). Clasps are CLIP-115 and -170 associating proteins involved in the regional regulation of microtubule dynamics in motile fibroblasts. Cell 104, 923–935.

Bergmann JE, Kupfer A, Singer SJ (1983). Membrane insertion at the leading edge of motile fibroblasts. Proc Natl Acad Sci USA 80, 1367–1371.

Bisel B, Wang Y, Wei JH, Xiang Y, Tang D, Miron-Mendoza M, Yoshimura S, Nakamura N, Seemann J (2008). ERK regulates Golgi and centrosome orientation towards the leading edge through GRASP65. J Cell Biol 182, 837–843.

Bryant DM, Datta A, Rodriguez-Fraticelli AE, Peranen J, Martin-Belmonte F, Mostov KE (2010). A molecular network for de novo generation of the apical surface and lumen. Nat Cell Biol 12, 1035–1045.

Chabin-Brion K, Marceiller J, Perez F, Settegrana C, Drechou A, Durand G, Pous C (2001). The Golgi complex is a microtubule-organizing organelle. Mol Biol Cell 12, 2047–2060.

Chen JL, Fucini RV, Lacomis L, Erdjument-Bromage H, Tempst P, Stamnes M (2005). Coatomer-bound Cdc42 regulates dynein recruitment to COPI vesicles. J Cell Biol 169, 383–389.

Cohen D, Musch A, Rodriguez-Boulan E (2001). Selective control of basolateral membrane protein polarity by cdc42. Traffic 2, 556–564.

Cole NB, Sciaky N, Marotta A, Song J, Lippincott-Schwartz J (1996). Golgi dispersal during microtubule disruption: regeneration of Golgi stacks at peripheral endoplasmic reticulum exit sites. Mol Biol Cell 7, 631–650.

Conde C, Caceres A (2009). Microtubule assembly, organization, and dynamics in axons and dendrites. Nature reviews. Neuroscience 10, 319–332.

de Anda FC, Pollarolo G, Da Silva JS, Camoletto PG, Feiguin F, Dotti CG (2005). Centrosome localization determines neuronal polarity. Nature 436, 704–708.

De Matteis MA, Luini A (2008). Exiting the Golgi complex. Nat Rev Mol Cell Biol 9, 273–284.

Drabek K, van Ham M, Stepanova T, Draegestein K, van Horssen R, Sayas CL, Akhmanova A, Ten Hagen T, Smits R, Fodde R, *et al.* (2006). Role of CLASP2 in microtubule stabilization and the regulation of persistent motility. Curr Biol 16, 2259–2264.

Drubin DG, Nelson WJ (1996). Origins of cell polarity. Cell 84, 335–344.

Dubois T, Paleotti O, Mironov AA, Fraisier V, Stradal TE, De Matteis MA, Franco M, Chavrier P (2005). Golgi-localized GAP for Cdc42 functions downstream of ARF1 to control Arp2/3 complex and F-actin dynamics. Nat Cell Biol 7, 353–364.

Efimov A, Kharitonov A, Efimova N, Loncarek J, Miller PM, Andreyeva N, Gleeson P, Galjart N, Maia AR, McLeod IX, *et al.* (2007). Asymmetric CLASP-dependent nucleation of noncentrosomal microtubules at the trans-Golgi network. Dev Cell 12, 917–930.

Egorov MV, Capestrano M, Vorontsova OA, Di Pentima A, Egorova AV, Mariggio S, Ayala MI, Tete S, Gorski JL, Luini A, *et al.* (2009). Faciogenital dysplasia protein (FGD1) regulates export of cargo proteins from the golgi complex via Cdc42 activation. Mol Biol Cell 20, 2413–2427.

Erickson JW, Zhang C, Kahn RA, Evans T, Cerione RA (1996). Mammalian Cdc42 is a brefeldin A-sensitive component of the Golgi apparatus. J Biol Chem 271, 26850–26854.

Etienne-Manneville S (2008). Polarity proteins in migration and invasion. Oncogene 27, 6970–6980.

Etienne-Manneville S, Hall A (2001). Integrin-mediated activation of Cdc42 controls cell polarity in migrating astrocytes through PKCzeta. Cell 106, 489–498.

Etienne-Manneville S, Hall A (2003). Cdc42 regulates GSK-3beta and adenomatous polyposis coli to control cell polarity. Nature 421, 753–756.

Farquhar MG, Palade GE (1998). The Golgi apparatus: 100 years of progress and controversy. Trends Cell Biol 8, 2–10.

Fukata M, Nakagawa M, Kaibuchi K (2003). Roles of Rho-family GTPases in cell polarisation and directional migration. Curr Opin Cell Biol 15, 590–597.

Funahashi Y, Namba T, Nakamuta S, Kaibuchi K (2014). Neuronal polarization in vivo: growing in a complex environment. Curr Opin Neurobiol 27C, 215–223.

Garrard SM, Capaldo CT, Gao L, Rosen MK, Macara IG, Tomchick DR (2003). Structure of Cdc42 in a complex with the GTPase-binding domain of the cell polarity protein, Par6. EMBO J 22, 1125–1133.

Glick BS, Nakano A (2009). Membrane traffic within the Golgi apparatus. Annu Rev Cell Dev Biol 25, 113–132.

Goldstein B, Macara IG (2007). The PAR proteins: fundamental players in animal cell polarization. Dev Cell 13, 609–622.

Harris KP, Tepass U (2010). Cdc42 and vesicle trafficking in polarized cells. Traffic 11, 1272–1279.

Honnappa S, Gouveia SM, Weisbrich A, Damberger FF, Bhavesh NS, Jawhari H, Grigoriev I, van Rijssel FJ, Buey RM, Lawera A, *et al.* (2009). An EB1-binding motif acts as a microtubule tip localization signal. Cell 138, 366–376.

Horikoshi Y, Suzuki A, Yamanaka T, Sasaki K, Mizuno K, Sawada H, Yonemura S, Ohno S (2009). Interaction between PAR-3 and the aPKC-PAR-6 complex is indispensable for apical domain development of epithelial cells. J Cell Sci 122, 1595–1606.

Hurtado L, Caballero C, Gavilan MP, Cardenas J, Bornens M, Rios RM (2011). Disconnecting the Golgi ribbon from the centrosome prevents directional cell migration and ciliogenesis. J Cell Biol 193, 917–933.

Iden S, Collard JG (2008). Crosstalk between small GTPases and polarity proteins in cell polarization. Nat Rev Mol Cell Biol 9, 846–859.

Infante C, Ramos-Morales F, Fedriani C, Bornens M, Rios RM (1999). GMAP-210, A cis-Golgi network-associated protein, is a minus end microtubule-binding protein. J Cell Biol 145, 83–98.

Itoh N, Nakayama M, Nishimura T, Fujisue S, Nishioka T, Watanabe T, Kaibuchi K (2010). Identification of focal adhesion kinase (FAK) and phosphatidylinositol 3-kinase (PI3-kinase) as Par3 partners by proteomic analysis. Cytoskeleton 67, 297–308.

Joberty G, Petersen C, Gao L, Macara IG (2000). The cell-polarity protein Par6 links Par3 and atypical protein kinase C to Cdc42. Nat Cell Biol 2, 531–539.

Kakeno M, Matsuzawa K, Matsui T, Akita H, Sugiyama I, Ishidate F, Nakano A, Takashima S, Goto H, Inagaki M, et al. (2014). Plk1 phosphorylates CLIP-170 and regulates its binding to microtubules for chromosome alignment. Cell Struct Function 39, 45–59.

Kroschewski R, Hall A, Mellman I (1999). Cdc42 controls secretory and endocytic transport to the basolateral plasma membrane of MDCK cells. Nat Cell Biol 1, 8–13.

Kumar P, Lyle KS, Gierke S, Matov A, Danuser G, Wittmann T (2009). GSK-3beta phosphorylation modulates CLASP-microtubule association and lamella microtubule attachment. J Cell Biol 184, 895–908.

Kupfer A, Louvard D, Singer SJ (1982). Polarization of the Golgi apparatus and the microtubule-organizing center in cultured fibroblasts at the edge of an experimental wound. Proc Natl Acad Sci USA 79, 2603–2607.

Lalli G (2009). RalA and the exocyst complex influence neuronal polarity through PAR-3 and aPKC. J Cell Sci 122, 1499–1506.

Li R, Gundersen GG (2008). Beyond polymer polarity: how the cytoskeleton builds a polarized cell. Nat Rev Mol Cell Biol 9, 860–873.

Lin D, Edwards AS, Fawcett JP, Mbamalu G, Scott JD, Pawson T (2000). A mammalian PAR-3-PAR-6 complex implicated in Cdc42/Rac1 and aPKC signalling and cell polarity. Nat Cell Biol 2, 540–547.

Lin YC, Chiang TC, Liu YT, Tsai YT, Jang LT, Lee FJ (2011). ARL4A acts with GCC185 to modulate Golgi complex organization. J Cell Sci 124, 4014–4026.

Lowe M (2011). Structural organization of the Golgi apparatus. Curr Opin Cell Biol 23, 85–93.

Luna A, Matas OB, Martinez-Menarguez JA, Mato E, Duran JM, Ballesta J, Way M, Egea G (2002). Regulation of protein transport from the Golgi complex to the endoplasmic reticulum by CDC42 and N-WASP. Mol Biol Cell 13, 866–879.

Martin-Belmonte F, Gassama A, Datta A, Yu W, Rescher U, Gerke V, Mostov K (2007). PTEN-mediated apical segregation of phosphoinositides controls epithelial morphogenesis through Cdc42. Cell 128, 383–397.

Matas OB, Martinez-Menarguez JA, Egea G (2004). Association of Cdc42/N-WASP/Arp2/3 signaling pathway with Golgi membranes. Traffic 5, 838–846.

Mellman I, Nelson WJ (2008). Coordinated protein sorting, targeting and distribution in polarized cells. Nat Rev Mol Cell Biol 9, 833–845.

Miller PM, Folkmann AW, Maia AR, Efimova N, Efimov A, Kaverina I (2009). Golgi-derived CLASP-dependent microtubules control Golgi organization and polarized trafficking in motile cells. Nat Cell Biol 11, 1069–1080.

Mimori-Kiyosue Y, Grigoriev I, Lansbergen G, Sasaki H, Matsui C, Severin F, Galjart N, Grosveld F, Vorobjev I, Tsukita S, Akhmanova A (2005). CLASP1 and CLASP2 bind to EB1 and regulate microtubule plus-end dynamics at the cell cortex. J Cell Biol 168, 141–153.

Musch A, Cohen D, Kreitzer G, Rodriguez-Boulan E (2001). cdc42 regulates the exit of apical and basolateral proteins from the trans-Golgi network. EMBO J 20, 2171–2179.

Nagai-Tamai Y, Mizuno K, Hirose T, Suzuki A, Ohno S (2002). Regulated protein-protein interaction between aPKC and PAR-3 plays an essential role in the polarization of epithelial cells. Genes Cells 7, 1161–1171.

Nakayama M, Goto TM, Sugimoto M, Nishimura T, Shinagawa T, Ohno S, Amano M, Kaibuchi K (2008). Rho-kinase phosphorylates PAR-3 and disrupts PAR complex formation. Dev Cell 14, 205–215.

Nalbant P, Hodgson L, Kraynov V, Toutchkine A, Hahn KM (2004). Activation of endogenous Cdc42 visualized in living cells. Science 305, 1615–1619.

Nishimura T, Kaibuchi K (2007). Numb controls integrin endocytosis for directional cell migration with aPKC and PAR-3. Dev Cell 13, 15–28.

Nishimura T, Yamaguchi T, Kato R, Yoshizawa M, Nabeshima Y, Ohno S, Hoshino M, Kaibuchi K (2005). PAR-6-PAR-3 mediates Cdc42-induced Rac activation through the Rac GEFs STEF/Tiam1. Nat Cell Biol 7, 270–277.

Pegtel DM, Ellenbroek SI, Mertens AE, van der Kammen RA, de Rooij J, Collard JG (2007). The Par-Tiam1 complex controls persistent migration by stabilizing microtubule-dependent front-rear polarity. Curr Biol 17, 1623–1634.

Petrie RJ, Doyle AD, Yamada KM (2009). Random versus directionally persistent cell migration. Nat Rev Mol Cell Biol 10, 538–549.

Qiu RG, Abo A, Steven Martin G (2000). A human homolog of the C. elegans polarity determinant Par-6 links Rac and Cdc42 to PKCzeta signaling and cell transformation. Curr Biol 10, 697–707.

Rodriguez-Boulan E, Kreitzer G, Musch A (2005). Organization of vesicular trafficking in epithelia. Nat Rev Mol Cell Biol 6, 233–247.

Rosse C, Formstecher E, Boeckeler K, Zhao Y, Kremerskothen J, White MD, Camonis JH, Parker PJ (2009). An aPKC-exocyst complex controls paxillin phosphorylation and migration through localised JNK1 activation. PLoS Biol 7, e1000235.

Sato K, Watanabe T, Wang S, Kakeno M, Matsuzawa K, Matsui T, Yokoi K, Murase K, Sugiyama I, Ozawa M, Kaibuchi K (2011). Numb controls E-cadherin endocytosis through p120 catenin with aPKC. Mol Biol Cell 22, 3103–3119.

Schmoranzer J, Fawcett JP, Segura M, Tan S, Vallee RB, Pawson T, Gundersen GG (2009). Par3 and dynein associate to regulate local microtubule dynamics and centrosome orientation during migration. Curr Biol 19, 1065–1074.

Sengupta D, Linstedt AD (2011). Control of organelle size: the Golgi complex. Annu Rev Cell Dev Biol 27, 57–77.

Shorter J, Warren G (2002). Golgi architecture and inheritance. Annu Rev Cell Dev Biol 18, 379–420.

Suzuki A, Ohno S (2006). The PAR-aPKC system: lessons in polarity. J Cell Sci 119, 979–987.

Takahashi M, Shibata H, Shimakawa M, Miyamoto M, Mukai H, Ono Y (1999). Characterization of a novel giant scaffolding protein, CG-NAP, that anchors multiple signaling enzymes to centrosome and the golgi apparatus. J Biol Chem 274, 17267–17274.

Tsvetkov AS, Samsonov A, Akhmanova A, Galjart N, Popov SV (2007). Microtubule-binding proteins CLASP1 and CLASP2 interact with actin filaments. Cell Motil Cytoskeleton 64, 519–530.

Vinogradova T, Paul R, Grimaldi AD, Loncarek J, Miller PM, Yampolsky D, Magidson V, Khodjakov A, Mogilner A, Kaverina I (2012). Concerted effort of centrosomal and Golgi-derived microtubules is required for proper Golgi complex assembly but not for maintenance. Mol Biol Cell 23, 820–833.

Wang S, Watanabe T, Matsuzawa K, Katsumi A, Kakeno M, Matsui T, Ye F, Sato K, Murase K, Sugiyama I, et al. (2012). Tiam1 interaction with the PAR complex promotes talin-mediated Rac1 activation during polarized cell migration. J Cell Biol 199, 331–345.

Watanabe T, Noritake J, Kakeno M, Matsui T, Harada T, Wang S, Itoh N, Sato K, Matsuzawa K, Iwamatsu A, et al. (2009). Phosphorylation of CLASP2 by GSK-3beta regulates its interaction with IQGAP1, EB1 and microtubules. J Cell Sci 122, 2969–2979.

Westermann P, Knoblich M, Maier O, Lindschau C, Haller H (1996). Protein kinase C bound to the Golgi apparatus supports the formation of constitutive transport vesicles. Biochem J 320, 651–658.

Wittmann T, Waterman-Storer CM (2005). Spatial regulation of CLASP affinity for microtubules by Rac1 and GSK3beta in migrating epithelial cells. J Cell Biol 169, 929–939.

Wu WJ, Erickson JW, Lin R, Cerione RA (2000). The gamma-subunit of the coatomer complex binds Cdc42 to mediate transformation. Nature 405, 800–804.

Yadav S, Puri S, Linstedt AD (2009). A primary role for Golgi positioning in directed secretion, cell polarity, wound healing. Mol Biol Cell 20, 1728–1736.

Yoshihama Y, Sasaki K, Horikoshi Y, Suzuki A, Ohtsuka T, Hakuno F, Takahashi S, Ohno S, Chida K (2011). KIBRA suppresses apical exocytosis through inhibition of aPKC kinase activity in epithelial cells. Curr Biol 21, 705–711.

Zmuda JF, Rivas RJ (1998). The Golgi apparatus and the centrosome are localized to the sites of newly emerging axons in cerebellar granule neurons in vitro. Cell Motil Cytoskeleton 41, 18–38.